Applied Biochemistry and Biotechnology (2022) 194:3765–3778
https://doi.org/10.1007/s12010-022-03931-7

ORIGINAL ARTICLE

Highly Sensitive Enzymatic Biosensor Based on Polyaniline-Wrapped Titanium Dioxide Nanohybrid for Fish Freshness Detection

Deeksha Thakur[1] · Chandra Mouli Pandey[1,2] · D. Kumar[1]

Accepted: 20 April 2022 /Published online: 6 May 2022

Abstract
Herein, we envisage the fabrication of a highly sensitive enzymatic electrochemical biosensor for selective detection of xanthine (Xn) using xanthine oxidase (XOs) immobilized polyaniline-wrapped titanium dioxide (PANI@TiO_2) nanohybrid as a sensing platform. The PANI@TiO_2 nanohybrid was synthesized via chemical polymerization using ammonium per sulfate as an oxidant. Various microscopic, spectroscopic, and electrochemical techniques have been utilized to confirm the electrophoretic deposition of the PANI and PANI@TiO_2 nanohybrids on to indium tin oxide (ITO) coated glass substrate. The fabricated XOs/PANI@TiO_2/ITO electrode exhibits enhanced electron transfer kinetics with an electron transfer rate constant of 0.904 cm s^{-1}. The electrochemical results show that the fabricated biosensor can detect Xn in the concentration range 1–100 μM, with a limit of detection of 0.1 μM ($S/N=3$) and a response time of 10 s. The validation of the biosensors has been conducted using real samples obtained from the *rohu* (*Labeo rohita*) fish. The proposed biosensor can be a reliable analytical tool for determining Xn concentration in commercial fish and meat samples.

Keywords Xanthine · Electrophoretic · Conducting polymers · Titanium dioxide · Biosensor

Introduction

There has been a significant increase in demand for fish as a nutritious and healthful food, and this has created an urgent need to detect its freshness [1]. After fish death, various autocatalytic reactions, decomposition of nucleotides, start immediately by

✉ Chandra Mouli Pandey
cmp.npl@gmail.com

✉ D. Kumar
dkumar@dce.ac.in

Deeksha Thakur
thakur.diksha2@gmail.com

[1] Department of Applied Chemistry, Delhi Technological University, Delhi 110042, India

[2] Department of Chemistry, Faculty of Science, Shree Guru Gobind Singh Tricentenary University, Gurugram 122505, Haryana, India

endogenous enzymes that are present in the intestine and muscle tissues [2]. The rapid degradation of adenosine triphosphate (ATP) results in increased concentration of inosine, which by bacterial metabolism is transferred to hypoxanthine and xanthine (Xn) [3]. Xn is a by-product of the degradation of nucleotides and its concentration increases with storage that causes a bitter taste in fish meat [4]. Xn is found as a constituent of nucleic acids and it accumulates not only in fish but also in human organs (heart, kidney, and skeletal muscle). The excess volume of Xn concentrations in human blood and urine may lead to various physiological issues such as gout, hyperuricemia, and preeclampsia [5, 6]. Therefore, there is an urgency for the detection of Xn as it is an indicator for fish freshness. The traditional methods commonly used for Xn determination are based on spectrophotometric and chromatographic techniques that require sample pretreatment, are time consuming, laborious, and may result in toxic waste [7]. The development of a quick, accurate, reliable, and cost-effective technique for determining fish freshness is a major requirement in the marine food industry [8–10]. The new analytical strategies may lead to the development of assay methods with anticipated reusability, portability, reversibility sensitivity, selectivity, simplicity, and the possibility to monitor a variety of parameters simultaneously. In this context, electrochemical biosensors can be used as promising alternative methods for faster, reliable, and simpler ways for detection of Xn [11, 12].

Conducting polymers (CPs) have aroused much research interest in the fabrication of biosensors because of their excellent physicochemical and electrical properties that can be tailored to specific needs. Electrochemical biosensors based on CPs are more affordable, simple to fabricate, and offer a direct electrical readout for recognizing natural analytes with exceptional sensitivity and selectivity [13]. Among the different CPs, polyaniline (PANI) has been widely used for the development of biosensors because of its ease of processing, long-term environmental stability, and functionality-rich chemical structure [14, 15]. Inspite of these advances, the main drawback of using PANI-based biosensors is their low response, low detection limit, and inadequate selectivity. Further, to improve the desired functional and structural properties of PANI such as high aspect ratio, enhanced mechanical strength, and electrical properties, it can be integrated with nanostructured metal oxides (NMOs). These NMOs provide a large surface area and multiple active sites for the immobilization of the biomolecules, which result in the efficient transfer of the electrons between the electrode and the electrolyte [16]. In this context, titanium dioxide (TiO_2) nanoparticles have aroused a lot of attention among various NMOs because of their exceptional properties such as outstanding surface-to-volume ratio, chemical stability, biocompatibility, ability to immobilize biomolecules, and exceptional thermoelectric capabilities [17–21]. The integration of PANI with TiO_2 nanoparticles can minimize the agglomeration of the nanoparticles, thus, improving the stability and allowing uniform dispersion in the polymer matrix [22, 23].

In this work, PANI@TiO_2 nanohybrid has been chemically synthesized using the oxidative polymerization technique. The synthesized PANI@TiO_2 nanohybrid has been used as an electrode material for the detection of Xn to evaluate fish freshness by depositing it electrophoretically onto indium tin oxide (ITO)-coated glass substrate. The validation of the fabricated biosensor was investigated in the real sample by determining the Xn concentration in the fish meat. The unique architecture of PANI@TiO_2 nanohybrid provides a large electro-active surface area, fast electron kinetics, and improved catalytic activity leading to enhanced electrochemical performance [16].

Materials and Methods

Chemicals

Titanium tetrachloride ($TiCl_4$), aniline (99.5% pure), hydrochloric acid (HCl, 0.5 M), and ammonium persulfate (APS, ≥ 98% pure) have been procured from Fisher-Scientific, India. Glutaraldehyde, xanthine oxidase (XOs, ≥ 7 units/mg protein), xanthine (≥ 99.5%), and other reagents and solvents were purchased from Sigma-Aldrich, USA. The solutions were prepared in double-distilled water (Milli-Q, Millipore, 18.2 MU) and the glasswares were autoclaved before use.

Synthesis of TiO_2 Nanoparticles

For nanostructured TiO_2, 1 mL of $TiCl_4$ was added to dilute H_2SO_4 (10%) solution in an ice bath with constant stirring. The solution turns grey due to the hydrolysis of $TiCl_4$. It was then held at 60 °C for heating until a clear solution was observed, and then aged for 1 h at room temperature. After that, 40 mL (drop by drop) of NH_4OH was added to the solution until the pH reached 7.0 and the solution turned white. The solution was allowed to cool and after that, it was washed and rinsed using DI water. The formed precipitate was vacuum dried and calcined at 400 °C, yielding an off-white tinted powder of TiO_2 nanoparticles [24, 25].

One-Pot Synthesis of PANI@TiO_2 Nanohybrid

The PANI@TiO_2 nanohybrid has been synthesized via a chemical approach using aniline as the monomer and APS as the oxidant. One milliliter of distilled aniline was dissolved in 0.5 M HCl in a 100 mL beaker. During the process, the beaker was set aside in an ice bath at a temperature of − 2 °C to − 4 °C for 10 h under constant stirring. After that, 1 mL of APS was added to the solution along with 0.2 mg of synthesized TiO_2 and kept in an ultrasonication bath for further dissolution. After 2 h of sonication, the solution was left undisturbed overnight at 4 °C. Further, the solution was rinsed and filtered using 2 M of HCl, and the resultant green-colored PANI@TiO_2 nanohybrid was dried at 60 °C for 24 h [26]. The same method was used to synthesize PANI without TiO_2 doping.

Electrophoretic Deposition (EPD) of PANI@TiO_2 Nanocomposite

The synthesized PANI@TiO_2 nanohybrid was deposited using the electrophoretic deposition (EPD) technique (Genetix, Model GX300C) onto a pre-hydrolyzed ITO electrode using a two-electrode system where platinum was taken as a counter-electrode. Both the electrodes were placed at a distance of 0.5 cm. The PANI@TiO_2 nanohybrid was sonicated in deionized water until a clear solution was obtained. For the deposition, 10 mL of the sonicated solution was diluted with 5 mL of ethanol and subjected to EPD. The deposition of the film at various voltages was carried out and the smooth film formation

was observed at 10 V and the time was 25 s. After the deposition, the prepared electrode was kept for drying.

Fabrication of PANI@TiO_2 Nanohybrid-Based Biosensor

For the immobilization of XOs, the PANI@TiO_2/ITO electrode was treated with 0.1% glutaraldehyde and left for 1 h at ambient temperature for the activation of the functional group present on the electrode surface [1]. Further, the electrode was washed with phosphate buffer saline (PBS; 100 mM, pH 7.4, 0.9% NaCl), followed by the covalent immobilization of XOs (20 µL). The electrode was kept overnight at room temperature in moist condition. The scheme for the synthesis of the PANI@TiO_2 nanohybrid and fabrication of the electrode is shown in Fig. 1.

Instrumentation

Bruker D-8 Advance X-ray diffractometer with monochromatic (Cu Kα) radiation ($\lambda = 1.5406$ A°) was used to record the X-ray diffraction (XRD) pattern in the 2θ range (10–80°) at a scan speed of 2°/min. To investigate the formation of PANI@TiO_2 nanohybrid, FT-IR measurements were performed using the Nicolet™ iS10 at a frequency range of 400–4000 cm^{-1}. Thermal studies were carried out to investigate the thermal degradation of the synthesized material in the temperature range of 25 °C to 1000 °C at the rate of 10 °C/min in a nitrogen environment using thermogravimetric analysis (TGA; Perkin-Elmer 4000). Scanning electron microscope (SEM, FEI NOVA NANOSEM 650) was used to analyze the surface morphology of PANI@TiO_2/ITO and XOs/PANI@TiO_2/ITO electrodes. The Autolab potentiostat/galvanostat (Eco-Chemie, the Netherlands) having a three-electrode system was used to perform electrochemical experiments with platinum as an auxiliary electrode

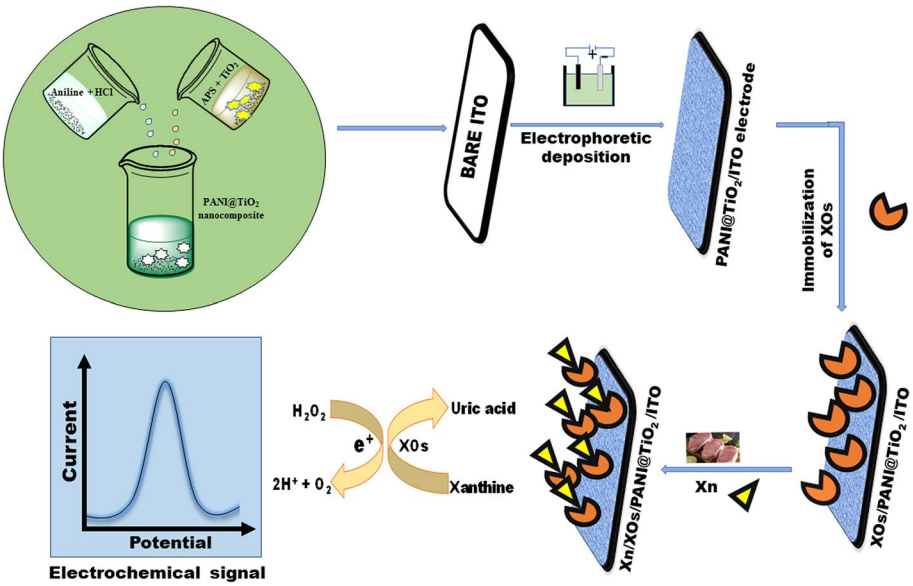

Fig. 1 Scheme showing the fabrication of PANI@TiO_2 nanohybrid–based biosensor

and Ag/AgCl as a reference electrode. All the electrochemical experiments were performed in phosphate buffer saline (PBS, 100 mM) pH 7.4 containing 5 mM $[Fe(CN)_6]^{3-/4-}$.

Results and Discussion

X-ray diffraction studies for PANI, TiO_2, and PANI@TiO_2 nanohybrid are shown in Fig. 2A. The broad reflection peak that appears around 20°–24° indicates that PANI was partially crystalline (curve (i)). The characteristic peaks at 25.5°, 38.14°, and 48.09° corresponded to the 101, 004, and 200 planes, respectively, confirming the presence of TiO_2 nanoparticles in PANI (curve (iii)). However, the pattern of the synthesized PANI@TiO_2 nanohybrid was found to be identical with TiO_2 (curve (ii)) and does not reflect any typical peak of PANI pattern. This may be due to the highly crystalline behavior of TiO_2 which overpower the intensity of the characteristic peaks of PANI [27].

The FT-IR spectra of PANI and PANI@TiO_2 nanohybrid displays benzenoid and quinonoid ring stretching bands at 1602 and 1482 cm^{-1}, respectively. The peaks at 2865 and 2853 cm^{-1} depict C–H stretching vibrations. Whereas, the bands at 1171, 1403, and 822 cm^{-1} are credited to C–N, C=N bond stretching, and C–H (benzene ring) out of the plane bending vibrations, respectively. The broad absorption bands (1000 to 550 cm^{-1}) is due to Ti–O–Ti vibration has been observed in PANI@TiO_2 nanohybrid, confirming the effective incorporation of TiO_2 into the PANI matrix (Fig. 2B (curve ii)) [28, 29].

The thermal stability of the nanohybrid has been studied using TGA. Figure 2C shows the mass losses of PANI and PANI@TiO_2 nanohybrids, heated at N_2 atmosphere. Initially,

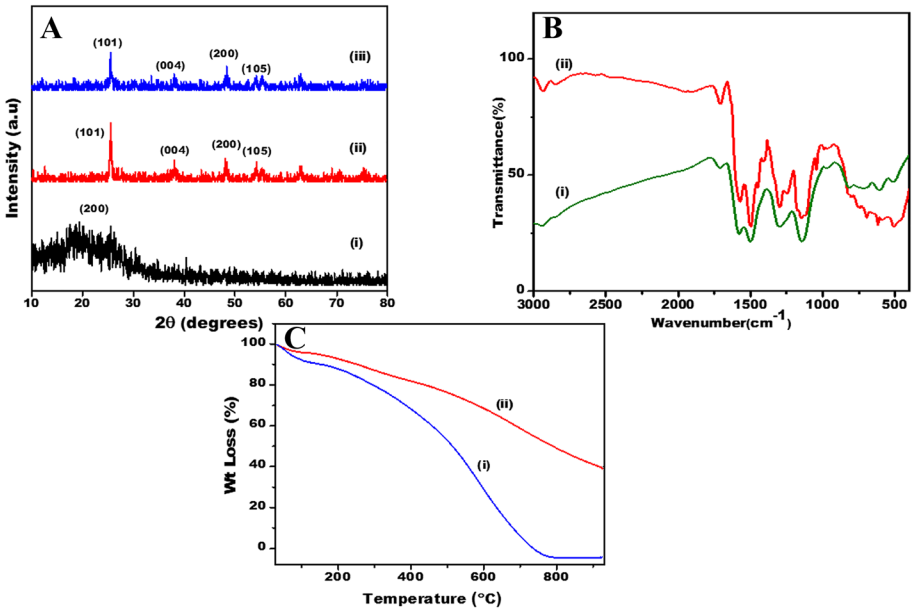

Fig. 2 **A** XRD of (i) PANI, (ii) TiO_2 nanoparticle, and (iii) PANI@TiO_2 nanohybrid; **B** FT-IR spectra of (i) PANI and (ii) PANI@TiO_2 nanohybrid; and **C** TGA curve for (i) PANI and (ii) PANI@TiO_2 nanohybrid in the range 25 °C–900 °C (10 °C/min), in a nitrogen environment

the loss in mass corresponds to the desorption of the moisture present in the material. PANI displays a rapid decrease in mass (10%) at a temperature of 280 °C due to the breakaway of dopant bonds (curve i). After that, a steady decrease in mass occurs in the range of 280 °C–600 °C. Whereas, the PANI@TiO_2 nanohybrid exhibits good stability with a slight loss in mass (4%) from 100 °C to 400 °C, and after 400 °C, the degradation rate increases (curve ii). The loss in mass of PANI may be due to the breakage of the polymer chain in the temperature range 280 °C to 600 °C. While the loss of mass in PANI@TiO_2 nanohybrid is slightly lower because TiO_2 restricts the flexibility of PANI chains, making them more stable than pristine PANI. The mass loss at 600 °C was found to be smaller for the PANI@TiO_2 nanohybrid, which indicates that the synthesized nanohybrid has good thermal behavior compared to the bare PANI [30].

The SEM image of PANI@TiO_2/ITO (Fig. 3A) shows that PANI@TiO_2 nanohybrid is evenly distributed on the surface of the ITO electrode [16]. After the immobilization of XOs on the PANI@TiO_2/ITO electrode, there was a structural change in the morphology, confirming that the enzyme has been evenly spread all over the PANI@TiO_2/ITO surface (Fig. 3B). Some globular-like structure observed in the SEM image is perhaps due to the agglomeration of XO on the surface of PANI@TiO_2/ITO electrode.

Electrochemical Studies of the Fabricated Electrodes

The electrochemical studies of bare ITO, PANI/ITO, and PANI@TiO_2/ITO electrodes have been performed using electrochemical impedance spectroscopy (EIS; PBS 5 mM of $[Fe(CN)_6]^{3-/4-}$) in the frequency range of 0.01–10^5 Hz [16]. In the Nyquist plot, a linear region is observed at lower frequencies and a semicircle region at higher frequencies, which corresponds to the diffusion-controlled electron transfer resistance process and electron transfer resistance–limited process, respectively [31]. The equivalent circuit (Fig. 4A (inset)) consists of solution resistance (R_s), an electron transfer resistance (R_{ct}), Warburg impedance (Z_w), and constant phase element (CPE) [18]. The R_{ct} of the ITO electrode was found to be 500.5 Ω (curve (i)), whereas the R_{ct} for PANI/ITO electrode and PANI@TiO_2/ITO electrode was found to be 123.9 Ω (curve (ii)) and 60.09 Ω (curve iii), respectively. The synergistic impact of PANI and TiO_2 provides a direct

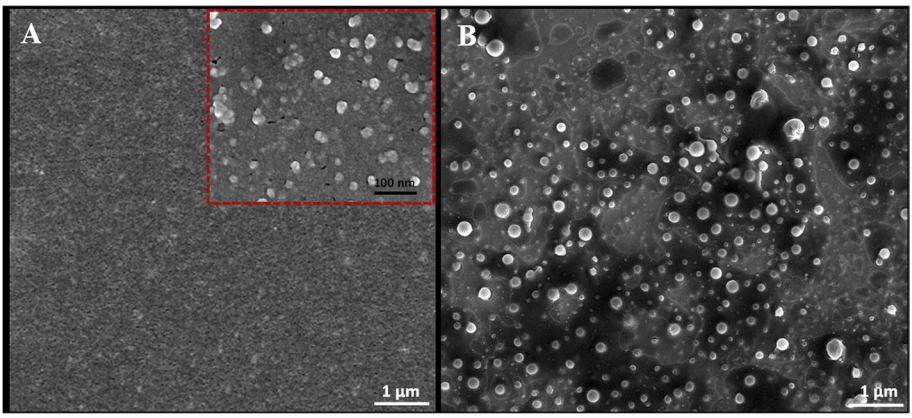

Fig. 3 SEM images of **A** PANI@TiO_2/ITO electrode and **B** XOs/PANI@TiO_2/ITO electrode

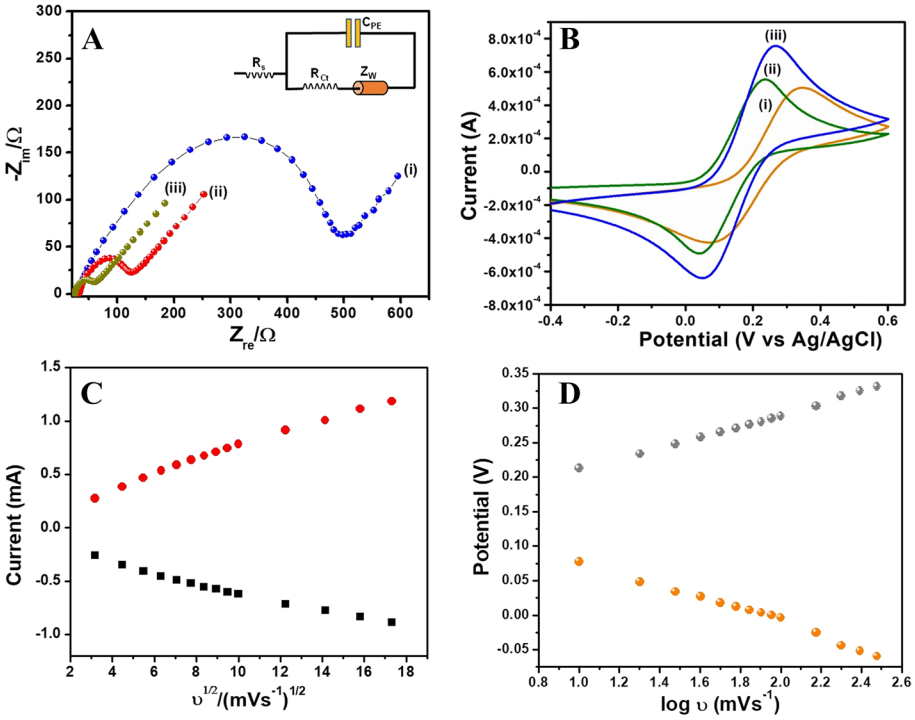

Fig. 4 **A** Nyquist diagram for the Faradic impedance for (i) ITO electrode, (ii) PANI/ITO electrode, and (iii) PANI@TiO_2/ITO electrode measured in PBS solution (pH 7) containing 5 mM $[Fe(CN)_6]^{3-/4-}$, in the frequency range from 10^5 to 10^{-2} Hz. **B** CV studies of (i) PANI/ITO electrode, (ii) PANI@TiO_2/ITO electrode, and (iii) XOs/PANI@TiO_2/ITO electrode. The plots of **C** I_{pa}, I_{pc} vs. square root of scan rate and **D** potential with log of scan rate with varying scan rate (10–300 mV) for PANI@TiO_2/ITO electrode

channel for charge transfer and a controlled diffusion process of the mediator ion, resulting in a lower R_{ct} value for the PANI@TiO_2/ITO electrode as compared to the PANI electrode [32].

From the obtained R_{ct} values, the electrochemical reaction that takes place at the electrode can be investigated by electron-transfer kinetics. The exchange current per geometric unit area (i_0) and apparent electron transfer rate constant (K_{app}) for PANI/ITO and PANI@TiO_2/ITO electrodes have been calculated using Eqs. (1) and (2).

$$i_0 = nRT/R_{ct}F \tag{1}$$

$$K_{app} = RT/n^2F^2AR_{ct}C \tag{2}$$

The i_0 for the PANI/ITO electrode was found to be 20.72×10^{-5} Acm^{-2}, whereas for the PANI@TiO_2/ITO electrode, i_0 calculated was 42.73×10^{-5} Acm^{-2}. Similarly, K_{app} for the PANI/ITO and PANI@TiO_2/ITO electrodes has been calculated to be 1.705×10^{-6} cm s^{-1} and 3.515×10^{-6} cm s^{-1}, respectively. This increase in values, i_0 and K_{app} of the PANI@TiO_2/ITO electrode compared to the PANI/ITO electrode, directly explains the precise diffusion of redox couple through the electrode interface [18].

Cyclic voltammetric studies have been carried out for PANI/ITO, PANI@TiO_2/ITO, and XOs/PANI@TiO_2/ITO electrodes in PBS buffer (Fig. 4B). It has been seen that the redox peak current of the PANI@TiO_2/ITO electrode (curve (ii); 0.49 mA) is higher compared to PANI/ITO electrode (curve (i)). It can be inferred that TiO_2 improves the conductivity of PANI@TiO_2/ITO electrode when compared to PANI/ITO electrode [33]. After the enzyme (XOs) is immobilized on PANI@TiO_2/ITO electrode, the redox peaks become more dominant (curve (iii); 2.02 mA) and the peak current value shifts to the positive side. This signifies that a direct electron pathway was taking place between the active site of XOs and the electrode, besides more enzymes are in interaction with the redox couple, thus indicating an increase in the oxidation signal [34].

The effect of changing the scan rate on the PANI@TiO_2/ITO electrode was explored, and it was observed that the rise in the scan rate from 10 to 300 mV/s resulted in a linear increase in oxidation peak current and a positive shift in the oxidation peak potential. Both the peak anodic (I_{pa}) and cathodic (I_{pc}) currents increases linearly with increasing scan rate and follow Equations (3) and (4), showing surface adsorption-controlled process kinetics (Fig. 4C).

$$Ipa(\mu A) = 1.2839 \times 10^{-4} + 6.3103 \times 10^{-5}\sqrt{v(mV/s)} \quad R = 0.9957 \tag{3}$$

$$Ipc(\mu A) = -1.7101 \times 10^{-4} - 4.2967 \times 10^{-5}\sqrt{v(mV/s)} \quad R = 0.9929 \tag{4}$$

Similarly, a linear correlation was observed for anodic and cathodic peak potentials (E_{pa} and E_{pc}) for increasing the natural logarithm of scan rate (ln$v$). The linear regression equations depicting the same have been given as Eqs. (5) and (6), respectively [35] (Fig. 4D).

$$Epa(V) = 0.1328\ln(v) + 0.0792; R = 0.9755 \tag{5}$$

$$Epc(V) = 0.1742ln(v) - 0.0928; R = 0.9868 \tag{6}$$

Using Laviron's model (Eq. 7), the charge transfer coefficient (α) and heterogeneous electron transfer coefficient (K_s) for PANI@TiO_2/ITO electrode have been calculated to be 0.9010 s^{-1} and 0.0772 s^{-1}, respectively, at a scan rate (v) of 50 mV/s.

$$ln(K_s) = \alpha ln(1-\alpha) + (1-\alpha)ln(\alpha) - ln(\frac{RT}{nFv}) - \alpha(1-\alpha)\frac{nF\Delta E_p}{RT} \tag{7}$$

Using linearity curves and Randles Sevick equation, Eq. (8), the diffusion coefficient (D) for the PANI@TiO_2/ITO electrode was found to be 5.48×10^{-11} cm^2 s^{-1}.

$$I_p = (2.99 \times 10^5)\alpha^{1/2}n^{3/2}ACD^{1/2}v^{1/2} \tag{8}$$

where C is the molar concentration of $[Fe(CN)_6]^{3-/4-}$ and A is the electrode area. The different kinetic parameters calculated for the PANI@TiO_2/ITO and XOs/PANI@TiO_2/ITO electrodes have been summarized in Table ST1. The observed improved electrochemical performance of the biosensor could be due to the improved conductivity of PANI@TiO_2 nanohybrid against bare PANI, which enhance the charge transfer rate and provides a single channel for interaction with the enzyme.

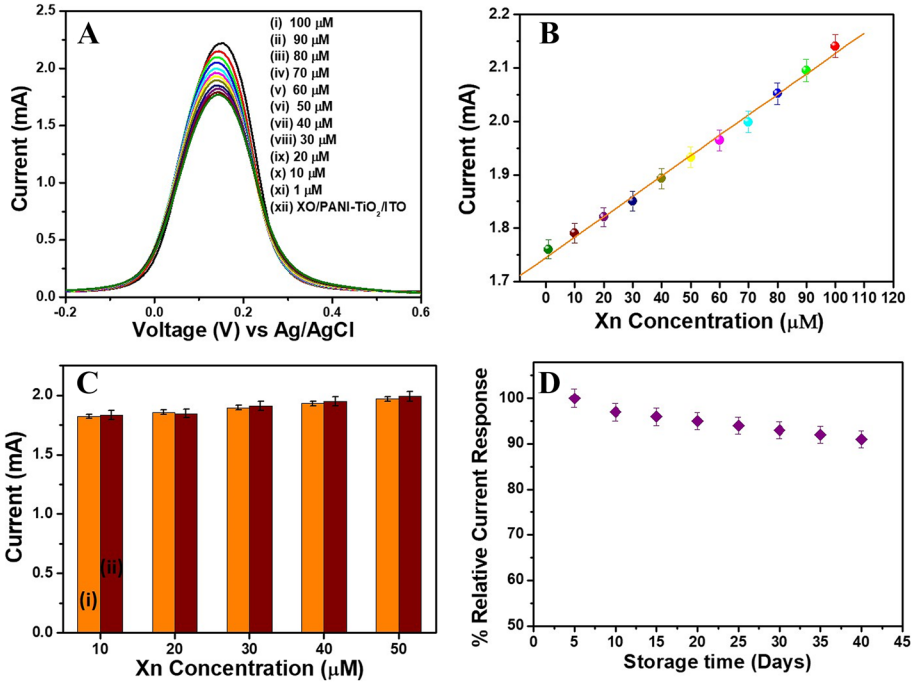

Fig. 5 **A** DPV studies showing the response of the XOs/PANI@TiO_2/ITO electrode with increasing concentration of Xn (from bottom to top, 1–100 µM); **B** calibration plot showing a linear relationship between the magnitudes of current recorded and concentration of Xn; **C** real sample analysis of biosensor with (i) buffer sample and (ii) real fish sample; and **D** stability studies of the fabricated biosensor

Electrochemical Biosensing Response Studies of XOs/PANI@TiO_2/ITO Electrode

The electrochemical biosensing studies of the XOs/PANI@TiO_2/ITO electrode have been carried out in the presence of different Xn concentrations (Fig. 5A). When the concentration of Xn was increased from 1 to 100 µM, the peak current response increased linearly. This increase in current indicates that there is a direct electron transfer between the Xn and the XOs/PANI@TiO_2/ITO electrode, which exhibits a good linear relationship between the Xn concentration and the current response (Fig. 5B). The sensitivity of the fabricated biosensor calculated using the regression equation: $y = 1.7704x + 0.4156$ (y = peak current and x = concentration of Xn) has been found to be 0.415 µA M^{-1} with $R^2 = 0.9942$. The limit of detection calculated using the Eq. $3\sigma/S$ was found to be 0.1 µM, where σ is standard deviation and S is the sensitivity obtained from the slope of the calibration curve [18].

Validation of the Biosensor with Real Sample

The practicality of the fabricated PANI@TiO_2/ITO biosensor for analyzing fish meat samples was conducted using DPV. The extraction of Xn from rohu (*Labeo rohita*) fish and the preparation of the Xn solution have been carried out using a simple method proposed by Watanabe et al [36]. In brief, fresh rohu fish was chopped and centrifuged at 4000 rpm in

Table 1 Comparison of the performance of PANI@TiO_2/ITO with other CP-based biosensors for Xn detection

S. No	Immobilization matrix	Detection technique	Linear range	LOD	Ref
1	Poly (L-aspartic acid)/MWCNT bio-nanocomposite	DPV	0.005–50.0 µM	3.5×10^{-4} µM	[38]
2	Polypyrrole films	Amperometry	4.0×10^{-4} M	1.0 µM	[39]
3	Poly (amino hydroxy naphthalene sulfonic acid)/GCE	LSV	4.0×10^{-4} -3.0×10^{-6} M	7.1×10^{-7} M	[40]
4	Polypyrrole-polyvinyl sulfonate film	Amperometry	10^{-7}–10^{-3} M	1.0×10^{-7} M	[36]
5	Nano-$CaCO_3$/GCE	CV	2×10^{-6}–2.5×10^{-4} M	2 µM	[41]
6	Ag-doped ZnO nanoparticles/polypyrrole	EIS Chronoamperometry	0.06–0.6 µM	0.07 µM	[42]
7	Graphene-TiO_2	CV	20–512 µM	9.5 µM	[43]
8	Poly-TTCA/Au	CV	5.0×10^{-6} – 1.0×10^{-4} M	1 µM	[44]
9	PANI@TiO_2/ITO	DPV	1–100 µM	0.1 µM	Present work

15-mL distilled water. Then the mixture was filtered using Whatman filter paper and was diluted 100 times to get the desired results. Electrochemical studies show that there was a continuous increase in the peak current with an increase in the Xn concentration from 10 to 50 μM and the results were similar to that of the synthetic Xn samples (Fig. 5C) [37]. The different biosensing parameters of the XOs/PANI@TiO_2-based biosensor were compared with previously reported polymer-based biosensors for Xn detection (Table 1), and it was observed that the fabricated biosensor shows an excellent response to Xn with low LOD and can detect the presence of Xn in fish meat sample. The proposed biosensor was used to detect the freshness of fish extract by evaluating the current response over a period of time span from 0 to 8 days at room temperature. As the storage duration of fish extract was extended, the level of xanthine increased, and it was almost six times higher on day 8 than it was on day 1 (Fig. S1).

Specificity, Reproducibility, and Stability Studies

The interference studies of the biosensor have been carried out by incubating the XOs/PANI@TiO_2 electrode with the same concentration of other interfering analytes (ascorbic acid, urea, and glucose). It was observed that there was no change in the current when the biosensor was subjected to other analytes revealing the specificity of the biosensor for Xn detection (Fig. S2). Further, the biosensor was also incubated with a mixture of the interfering analytes containing Xn. The electrochemical results indicate that the biosensor was able to detect the presence of Xn even in the presence of other interfering analytes. The reproducibility of the fabricated biosensor has also been measured by a series of repetitive voltammetric analyses. The % recoveries calculated for the XOs/PANI@TiO_2/ITO electrode ranged from 96 to 99%, with an RSD value of ≈ 4% ($n=4$), which was obtained for a 10-μM Xn measurement, demonstrating the fabricated biosensor shows acceptable reproducibility. The stability of the XOs/PANI@TiO_2/ITO electrode was tested by monitoring the DPV response of the bioelectrode ($n=3$) to Xn (10 μM) every 5 days while it was stored at 4 °C. After 45 days of use, the biosensor lost around 8% of its original activity, indicating that the biosensor is stable for at least 40 days when stored at 4 °C in a dry state (Fig. 5D).

Conclusion

An electrochemical enzymatic biosensor has been developed for Xn detection using PANI@TiO_2 nanohybrid. The fabricated biosensor shows improved electrochemical properties, a reasonable detection limit (0.1 μM), and quick response time (10 s). The validation of the biosensor with real sample obtained from rohu fish shows its potential for field applications for detection of Xn in fish meat. The fabricated biosensor was found to be specific, stable (40 days), and reproducible. The developed PANI@TiO_2 nanohybrid–based platform has been successfully validated with the fish meat sample, which shows its applicability and reliability for fish freshness detection.

Abbreviations MWCNT: Multiwalled carbon nanotubes; XO: Xanthine oxidase; $CaCO_3$: Calcium carbonate; GCE: Glassy carbon electrode; Ag: Silver; ZnO: Zinc oxide; poly-TTCA: Poly-5,2′:5′,2″-terthiophine-3-carboxylic acid; Au: Gold; TiO_2: Titanium dioxide; ITO: Indium tin oxide; DPV: Differential pulse voltammetry; CV: Cyclic voltammetry; EIS: Electrochemical impedance spectroscopy

Supplementary Information The online version contains supplementary material available at https://doi.org/10.1007/s12010-022-03931-7.

Acknowledgements Deeksha acknowledges DST-INSPIRE for the SRF Award. C.M. Pandey acknowledges the Department of Science and Technology (DST), New Delhi, India for the DST-INSPIRE Faculty award.

Author Contribution Deeksha: conceptualization, methodology, data curation, formal analysis, writing—original draft. CMP: supervision, investigation, validation, writing—review and editing, funding acquisition. DK: supervision, validation, project administration, writing—review and editing.

Data Availability Not applicable.

Declarations

Ethics Approval Not applicable.

Consent to Participate Not applicable.

Consent for Publication Not applicable.

Competing Interests The authors declare no competing interests.

References

1. Kamil Reza, K., Singh, M. K., Yadav, S. K., Singh, J., Agrawal, V. V., & Malhotra, B. D. (2013). Quantum dots based platform for application to fish freshness biosensor. *Sensors and Actuators B: Chemical, 177*, 627–633.
2. Sahyar, B. Y., Kaplan, M., Ozsoz, M., Celik, E., & Otles, S. (2019). Electrochemical xanthine detection by enzymatic method based on Ag doped ZnO nanoparticles by using polypyrrole. *Bioelectrochemistry, 130*, 107327.
3. Devi, R., Yadav, S., & Pundir, C. S. (2011). Electrochemical detection of xanthine in fish meat by xanthine oxidase immobilized on carboxylated multiwalled carbon nanotubes/polyaniline composite film. *Biochemical Engineering Journal, 58–59*, 148–153.
4. Albelda, J. A. V., Uzunoglu, A., Santos, G. N. C., & Stanciu, L. A. (2017). Graphene-titanium dioxide nanocomposite based hypoxanthine sensor for assessment of meat freshness. *Biosensors and Bioelectronics, 89*, 518–524.
5. Lawal, A. T., & Adeloju, S. B. (2009). Comparison of enzyme immobilisation methods for potentiometric phosphate biosensors. *Biosensors and Bioelectronics, 25*, 406–410.
6. Ghanbari, K., & Nejabati, F. (2020). Ternary nanocomposite-based reduced graphene oxide/chitosan/Cr2O3 for the simultaneous determination of dopamine, uric acid, xanthine, and hypoxanthine in fish meat. *Analytical Methods, 12*, 1650–1661.
7. Jalil, O., Pandey, C. M., & Kumar, D. (2020). Electrochemical biosensor for the epithelial cancer biomarker EpCAM based on reduced graphene oxide modified with nanostructured titanium dioxide. *Microchimica Acta, 187*, 275.
8. Yadav, S. K., Singh, J., Agrawal, V. V., & Malhotra, B. D. (2012). Nanostructured nickel oxide film for application to fish freshness biosensor. *Applied Physics Letters, 101*, 023703.
9. Solanki, S., Pandey, C. M., Gupta, R. K., & Malhotra, B. D. (2020). Emerging trends in microfluidics based devices. *Biotechnology Journal, 15*, 1900279.
10. Xue, G., Yu, W., Yutong, L., Qiang, Z., Xiuying, L., Yiwei, T., & Jianrong, L. (2019). Construction of a novel xanthine biosensor using zinc oxide (ZnO) and the biotemplate method for detection of fish freshness. *Analytical Methods, 11*, 1021–1026.
11. Gerard, M., Chaubey, A., & Malhotra, B. D. (2002). Application of conducting polymers to biosensors. *Biosensors & Bioelectronics, 17*, 345–359.
12. Kumar, A. S., & Shanmugam, R. (2011). Simple method for simultaneous detection of uric acid, xanthine and hypoxanthine in fish samples using a glassy carbon electrode modified with as commercially received multiwalled carbon nanotubes. *Analytical Methods, 3*, 2088–2094.

13. Pundir, C. S., & Devi, R. (2014). Biosensing methods for xanthine determination: A review. *Enzyme and Microbial Technology, 57*, 55–62.
14. Dhand, C., Das, M., Datta, M., & Malhotra, B. D. (2011). Recent advances in polyaniline based biosensors. *Biosensors & Bioelectronics, 26*, 2811–2821.
15. Ahuja, T., Mir, I. A., Kumar, D., & Rajesh. (2007). Biomolecular immobilization on conducting polymers for biosensing applications. *Biomaterials, 28*, 791–805.
16. Soni, A., Pandey, C. M., Pandey, M. K., & Sumana, G. (2019). Highly efficient polyaniline-MoS2 hybrid nanostructures based biosensor for cancer biomarker detection. *Analytica Chimica Acta, 1055*, 26–35.
17. Solanki, P., Kaushik, A., Agrawal, V., & Malhotra, B. (2011). Nanostructured metal oxide-based biosensors. *NPG Asia Materials, 3*, 17–24.
18. Jalil, O., Pandey, C. M., & Kumar, D. (2021). Highly sensitive electrochemical detection of cancer biomarker based on anti-EpCAM conjugated molybdenum disulfide grafted reduced graphene oxide nanohybrid. *Bioelectrochemistry, 138*, 107733.
19. Verma, R., Samdarshi, S. K., Sagar, K., & Konwar, B. K. (2017). Nanostructured bi-phasic TiO2 nanoparticles grown on reduced graphene oxide with high visible light photocatalytic detoxification. *Materials Chemistry and Physics, 186*, 202–211.
20. Teli, S. B., Molina, S., Sotto, A., Calvo, E. G., & Abajob, J. D. (2013). Fouling resistant polysulfone–PANI/TiO2 ultrafiltration nanocomposite membranes. *Industrial & Engineering Chemistry Research, 52*, 9470–9479.
21. Xie, S., Gan, M., Ma, L., Li, Z., Yan, J., Yin, H., Shen, X., Xu, F., Zheng, J., Zhang, J., & Hu, J. (2014). Synthesis of polyaniline-titania nanotube arrays hybrid composite via self-assembling and graft polymerization for supercapacitor application. *Electrochimica Acta, 120*, 408–415.
22. Soni, A., Pandey, C. M., Solanki, S., Kotnala, R. K., & Sumana, G. (2018). Electrochemical genosensor based on template assisted synthesized polyaniline nanotubes for chronic myelogenous leukemia detection. *Talanta, 187*, 379–389.
23. Katoch, A., Burkhart, M., Hwang, T., & Kim, S. S. (2012). Synthesis of polyaniline/TiO2 hybrid nanoplates via a sol–gel chemical method. *Chemical Engineering Journal, 192*, 262–268.
24. Rab, N., Chong, F. K., Mohamed, H. I., & Lim, W. H. (2018). Preparation of TiO2 nanoparticles by hydrolysis of TiCl4 using water and glycerol solvent system. *Journal of Physics: Conference Series, 1123*, 012065.
25. Paul, G., Verma, S., Jalil, O., Thakur, D., Pandey, C. M., & Kumar, D. (2021). PEDOT: PSS-grafted graphene oxide-titanium dioxide nanohybrid-based conducting paper for glucose detection. *Polymers for Advanced Technologies, 32*, 1774–1782.
26. Elakkiya, S., Arthanareeswaran, G., Ismail, A. F., Das, D. B., & Suganya, R. (2019). Polyaniline coated sulfonated TiO2 nanoparticles for effective application in proton conductive polymer membrane fuel cell. *European Polymer Journal, 112*, 696–703.
27. Yu, H., Jang, K., Chung, I., & Ahn, H. (2016). Fabrication and electrochemical characterization of polyaniline/titanium oxide nanoweb composite electrode for supercapacitor application. *Journal of Nanoscience and Nanotechnology, 16*, 2937–2943.
28. Najafi, V., Ahmadi, E., Ziaee, F., Omidian, H., & Sedaghat, H. (2019). Polyaniline-modified TiO2, a highly effective photo-catalyst for solid-phase photocatalytic degradation of PVC. *Journal of Polymers and the Environment, 27*, 784–793.
29. Ahmad, R., & Mondal, P. K. (2012). Adsorption and photodegradation of methylene blue by esing PANI/TiO2 nanocomposite. *Journal of Dispersion Science and Technology, 33*, 380–386.
30. Emran, K. (2018). The electrocatalytic activity of polyaniline/TiO2 nanocomposite for Congo red degradation in Aqueous solutions. *International Journal of Electrochemical Science, 13*, 5085–5095.
31. Abaci, S., Nessark, B., & Riahi, F. (2014). Preparation and characterization of polyaniline+TiO2 composite films. *Ionics, 20*, 1693–1702.
32. Reddy, R., kv, K., S B, B., Soni, S., Jeong, H. M., and Anjanapura, R. (2016). Enhanced photocatalytic activity of nanostructured titanium dioxide/polyaniline hybrid photocatalysts. *Polyhedron, 120*, 169–174.
33. Majumdar, S., & Mahanta, D. (2020). Deposition of an ultra-thin polyaniline coating on a TiO2 surface by vapor phase polymerization for electrochemical glucose sensing and photocatalytic degradation. *RSC Advances, 10*, 17387–17395.
34. Elgrishi, N., Rountree, K. J., McCarthy, B. D., Rountree, E. S., Eisenhart, T. T., & Dempsey, J. L. (2018). A Practical beginner's guide to cyclic voltammetry. *Journal of Chemical Education, 95*, 197–206.

35. Pandey, C. M., Sumana, G., & Tiwari, I. (2014). Copper oxide assisted cysteine hierarchical structures for immunosensor application. *Applied Physics Letters, 105*, 103706.
36. Dolmacı, N., Çete, S., Arslan, F., & Yaşar, A. (2012). An amperometric biosensor for fish freshness detection from xanthine oxidase immobilized in polypyrrole-polyvinylsulphonate film. *Artificial Cells, Blood Substitutes, and Biotechnology, 40*, 275–279.
37. Narang, J., Malhotra, N., Singhal, C., Singh, M., & Pundir, C. (2016). Impedimetric and voltammetry sensing of xanthine using nanocomposites. *Advanced Materials Letters, 7*, 555–560.
38. Yazdanparast, S., Benvidi, A., Abbasi, S., & Rezaeinasab, M. (2019). Enzyme-based ultrasensitive electrochemical biosensor using poly(l-aspartic acid)/MWCNT bio-nanocomposite for xanthine detection: A meat freshness marker. *Microchemical Journal, 149*, 104000.
39. Arslan, F., Yaşar, A., & Kiliç, E. (2006). An amperometric biosensor for xanthine determination prepared from xanthine oxidase immobilized in polypyrrole film. *Artificial Cells, Blood Substitutes, and Immobilization Biotechnology, 34*, 111–126.
40. Mathew, M. R., & Girish Kumar, K. (2020). Poly(amino hydroxy naphthalene sulphonic acid) modified glassy carbon electrode; an effective sensing platform for the simultaneous determination of xanthine and hypoxanthine. *Journal of The Electrochemical Society, 167*, 047519.
41. Shan, D., Wang, Y., Xue, H., & Cosnier, S. (2009). Sensitive and selective xanthine amperometric sensors based on calcium carbonate nanoparticles. *Sensors and Actuators B: Chemical, 136*, 510–515.
42. Sahyar, B., Kaplan, M., Ozsoz, M., Celik, E., & Otles, S. (2019). Electrochemical xanthine detection by enzymatic method based on Ag doped ZnO nanoparticles by using polypyrrole. *Bioelectrochemistry, 130*, 107327.
43. Albelda, J. A. V., Uzunoglu, A., Santos, G. N. C., & Stanciu, L. A. (2017). Graphene-titanium dioxide nanocomposite based hypoxanthine sensor for assessment of meat freshness. *Biosensors and Bioelectronics, 89*, 518–524.
44. Rahman, M. A., Won, M.-S., & Shim, Y.-B. (2007). Xanthine sensors based on anodic and cathodic detection of enzymatically generated hydrogen peroxide. *Electroanalysis, 19*, 631–637.